Journal of
Marine Science
and Engineering

MDPI

*Article*

# Channel Model and Signal-Detection Algorithm for the Combined Effects of Turbulence and Link Misalignment in Underwater Optical Massive MIMO Systems

**Jielin Fu [1], Kongliang Zhu [1], Syed Agha Hassnain Mohsan [2], Yanlong Li [1,*]**

[1] Ministry of Education Key Laboratory of Cognitive Radio and Information Processing, School of Information and Communication, Guilin University of Electronic Technology, Guilin 541004, China
[2] Optical Communication Laboratory, Ocean College, Zhejiang University, Zheda Road 1, Zhoushan 316021, China
* Correspondence: lylong@guet.edu.cn

**Abstract:** In recent years, underwater wireless optical communication (UWOC) has become a potential wireless carrier candidate for signal transmission in water mediums such as oceans. Underwater signal transmission is impaired by several challenges such as turbulence, scattering, attenuation, and misalignment. In this paper, we propose an improved-order successive interference cancellation (I-OSIC) algorithm based on partition space–time block coding (STBC) technology to solve the sub-channel correlation enhancement problem, which is caused by the combined effects of turbulence and link misalignment in the underwater optical massive multiple-input multiple-output (massive MIMO) systems. The partition STBC technology can make the encoded symbols orthogonality of space and time resist random fading under turbulence environments and fully use the communication link of the massive MIMO system. Under link misalignment conditions, the receiver detector will receive multiple beams. The proposed I-OSIC algorithm based on partition STBC can precisely track the degree of link misalignment error and reorder receiver signals based on the minimum interference criterion. It can use the channel matrix to estimate the interference magnitude of the link misalignment, and then eliminate the interference successively by demodulating the least interfered signal first. When the link misalignment error is large, the I-OSIC algorithm can provide a signal-to-noise ratio (SNR) gain of about 3 dB and provides the same error performance compared with the successive interference cancellation algorithm based on the received signal power.

**Keywords:** massive MIMO; turbulence; link misalignment; OSIC; STBC



**Citation:** Fu, J.; Zhu, K.; Mohsan, S.A.H.; Li, Y. Channel Model and Signal-Detection Algorithm for the Combined Effects of Turbulence and Link Misalignment in Underwater Optical Massive MIMO Systems. *J. Mar. Sci. Eng.* **2023**, *11*, 547. https://doi.org/10.3390/jmse11030547

Academic Editor: Rafael Morales

Received: 13 February 2023
Revised: 27 February 2023
Accepted: 1 March 2023
Published: 3 March 2023



## 1. Introduction

In recent years, with the continuous intensification of global climate changes and the depletion of resources, research on oceanic detection systems has gained significant attention. With the increase in marine exploration, environmental monitoring, scientific research, marine safety, and other marine activities, an urgent need has emerged as high-speed, reliable, and powerful wireless communication technology. At present, underwater acoustic communication is still the most widely used underwater wireless communication technology, due to its long transmission distance and tolerance to water turbulence [1]. However, the data rate of underwater acoustic communication systems is still limited to the kbps level [2]. In addition, sound waves travel through water at a speed of 1480 m per second, which results in huge delays in underwater acoustic communication systems [3]. Radio frequency (RF) wireless communication technology [4,5] can significantly improve the data rate and latency of current underwater wireless communication systems. However, RF signals have excessive propagation loss in water [6,7]. Therefore, the transmission range of underwater RF systems is severely limited to less than 1 m [8]. Blue and green light with wavelengths between 450 and 550 nanometers are less attenuated by seawater.

The underwater wireless optical communication (UWOC) technology based on the blue and green light bands has the advantages of a high bandwidth and low delay over its counterparts, and can be used as a powerful supplement to underwater acoustic communication to realize short-distance and high data-rate underwater communication [9].

UWOC has gained a considerable attraction in research fraternity because of its potential to achieve high data rates over medium distances [10,11]. In the past few years, innovative breakthroughs in UWOC have been driven by light sources with higher power levels and transmission efficiency, photodetectors with higher sensitivity, and advanced coding schemes [12]. Laser diodes (LDs) [13,14] and light-emitting diodes (LEDs) [15,16] are commonly used as optical sources for UWOC applications. Compared with LDs, LEDs have the advantages of low cost, high power efficiency, and long life, but the narrow modulation bandwidth of LED limits the improvement of communication rate. To maximize the improvement of the communication rate, the massive multiple-input multiple-output (massive MIMO) technologies in the RF-based communication system are applied to the UWOC system [17].

However, the achievable rate of massive MIMO is limited due to channel correlation [18,19]. In UWOC systems, the problem of channel correlation is crucial due to the dominant line-of-sight (LOS) component [20]. Therefore, even $16 \times 16$ MIMO and $36 \times 36$ MIMO have been considered as massive MIMO systems [18]. Furthermore, the inter-channel interference (ICI) in underwater optical massive MIMO systems is higher due to the high spatial channel correlation. In the underwater optical massive MIMO systems, an imaging structure can be employed at the receiver side to achieve spatial diversity. Hemispherical lenses [21] and fish-eye lenses [22] are usually preferred to provide a wider field of view (FoV) while increasing optical gain, splitting beams, and reducing interference between different LED beams.

In the actual underwater short-range optical communication scenario, the relative motion caused by ocean currents resulting in the communication link to achieve accurate alignment is complex. Link misalignment will cause the detector to receive interference signals from adjacent LEDs, resulting in increased channel correlation. To solve the problem of aggravated interference between spot arrays, some scholars adopted the scheme of maximum ratio combining based on successive interference cancellation (MRC-SIC) [23]. However, this scheme is only applicable to such situations where the degree of link misalignment is small. It cannot mitigate the problem of signal loss when the imaging light spot deviates from the range of the detector under the condition of large link misalignment.

In addition, high power losses and random fading caused by absorption, scattering, turbulence, and other factors in the underwater environment are also major factors limiting the communication distance and reliability performance improvement of the UOWC system. To reduce the influence of turbulence on UOWC, spatial diversity technology can be used [24]. Space-time block coding (STBC) can alleviate the random attenuation of optical signals in turbulent environments [25]. STBC coding technology can also be applied to MIMO UWOC systems. The STBC coding technology ensures that the encoded symbols have orthogonality in space [26]. To reduce the receiver's complexity, the STBC coding technology and equal gain combined (EGC) technology can be adopted as viable approaches [27].

In this paper, our main contributions can be listed as follows.

- Establishing an underwater optical massive MIMO system model.
- Under the combined effects of turbulence and link misalignment, the underwater channel model of the underwater optical massive MIMO system is established.
- An improved-order successive interference cancellation (I-OSIC) algorithm based on partition STBC is proposed to solve the problem of enhanced interference between sub-channels caused by the combined effects of turbulence and link misalignment.
- Based on the characteristic of single offset direction of imaging spot, a SIC algorithm with a minimum interference sorting criterion is proposed.

Compared with the the OSIC algorithm based on signal power, it can effectively reduce the impact caused by the combined effect of turbulence and link misalignment.

The problem of system sub-channel correlation enhancement under the combined influence of turbulence and link misalignment is considered. Under the combined effects of turbulence and link misalignment, the underwater channel model of the underwater optical massive MIMO system is established. An I-OSIC algorithm based on partition STBC is proposed to solve the problem of enhanced interference between sub-channels caused by the combined effects of turbulence and link misalignment. Based on the characteristic of the single offset direction of the imaging spot, the SIC is carried out using the minimum interference sorting criterion. Compared with the OSIC algorithm based on signal power, it can effectively reduce the impact caused by the combined effect of turbulence and link misalignment.

The remainder of this paper is organized as follows. Section 2 describes the underwater optical massive MIMO system. Then we discuss the channel model under the combined effects of turbulence and link misalignment. Section 3 proposes the I-OSIC algorithm based on partition STB. Simulation results and discussions are provided in Section 4. Finally, we conclude this work in Section 5.

## 2. System Model

As shown in Figure 1, this paper uses a 16 × 16 MIMO system model for research and analysis. The transmitter consists of a matrix array of 16 LED light sources, and the receiver includes a lens group and 16 rectangular detectors. The sixteen LEDs on the transmitter side are divided into four groups of light sources, and each group of light sources is composed of four LEDs. The data transmitted by four LEDs in each group of light sources is encoded by STBC technology, and four light sources transmit four different signals, respectively. The modulated signal is converted into optical emission through the LED at the transmitter and the underwater channel. Arrays of lenses separate the beams between different LEDs at the receiver to reduce correlations between underwater sub-channels. In addition, the I-OSIC detection algorithm can further reduce the correlation between sub-channels under the link misalignment.

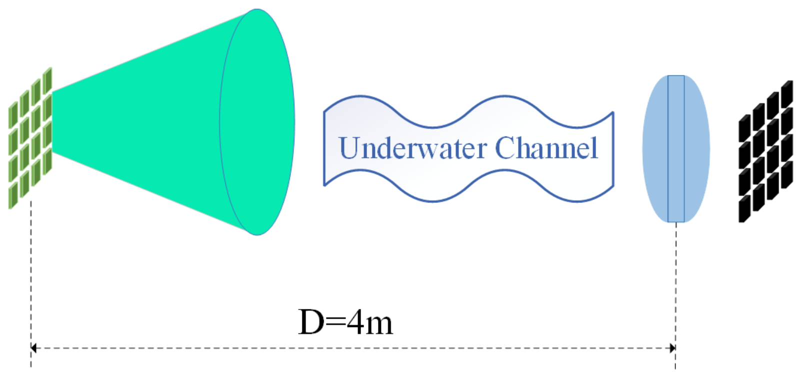


**Figure 1.** Model of underwater imaging optical communication system.

### 2.1. Underwater Optical Imaging MIMO-ACO-OFDM System

Figure 2 shows the block diagram of the system combining STBC coding technology and OFDM modulation technology. As shown in Figure 2, the system's transmitter is composed of $N_t$ LEDs, and the receiver of $N_r$ detectors. The binary bit stream is subjected to QAM mapping in order to obtain QAM symbols. The QAM symbols are STBC encoded and then modulated by asymmetric clipped OFDM (ACO-OFDM) to obtain OFDM symbols. Finally, they are converted into optical signals by LED after performing the clipping process. After receiving the optical signal at the receiver, four large light spots are obtained by imaging through the imaging lens. The signals received by each detector are estimated by channel, and then the detectors covered by light spots are combined using the EGC technique.

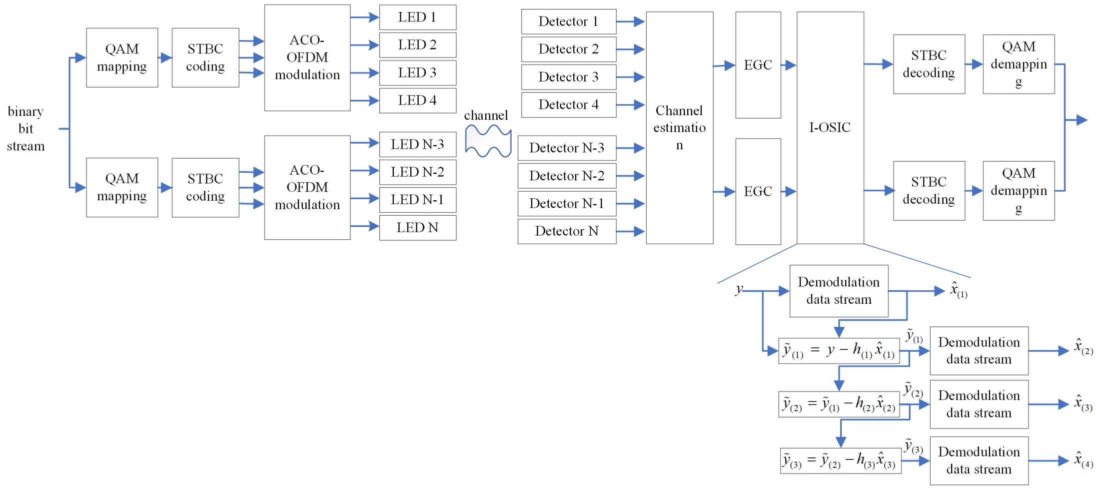


**Figure 2.** MIMO ACO-OFDM STBC system block diagram.

The variation of link distance between transmitter and receiver will also affect the size of the imaging spot. When the communication link is longer, the area of imaging spot and the distance between different spots will be smaller. On the contrary, if the communication distance is shorter, the imaging spot area will be larger and the interference between different spots will be larger. The imaging spot will be affected only when the communication link size changes to the magnitude of m. Therefore, this paper mainly analyzes and studies the relatively sensitive horizontal migration of the system.

Under the combined effects of turbulence and link misalignment, the underwater optical massive MIMO system is not only hindered by random fading but also the image spot of the receiver will be offset with the direction of link misalignment. The offset direction of the imaging spot of the receiver is single. Therefore, the beam received by the edge detector in the opposite direction of the receiver's spot offset is also single. The I-OSIC detection algorithm is used for the combined received signal to mitigate the interference of the previous signal. The receiver demodulates the received signal directly, uses the direct demodulated signal to finish interference cancellation, and finally demodulates the remaining signal as its data. As shown in Figure 2, the signal with weaker interference is $x_1$, so the first output is $x_{(1)}$ by direct detection. Signal can be recovered after the estimation of the signal with stronger interference and subtract it from the received signal $y$. Therefore, the next level input can be expressed as $h_{(1)}x_{(1)}$, the second output is $x_{(2)}$, where $h_{(i)}$ is the channel gain between the emitting LED and the $i$-th detector. The user detection order is a key point in the I-OSIC signal detection process. Here, the sequencing is performed based on the signal interference of the detectors. Finally, the received binary bit stream data is obtained through ACO-OFDM demodulation, STBC decoding, and QAM demapping.

### 2.2. Underwater Imaging Optical MIMO Channel Model

Seawater contains several inorganic salts, minerals, chlorophyll, etc. These suspended particles have a scattering effect on the direction of photon motion and an absorption effect on photon energy. The sum of the two effects represents the total attenuation coefficient of seawater to light. The simulated environment of the system is the pure ocean water, the total attenuation coefficient of visible light is $c(\lambda) = 0.15$ [14], and the channel DC gain $h_{ij}$ of the underwater optical massive MIMO system can be calculated by the following formula [28]:

$$h_{ij} = \eta_t \eta_r A_{eff}(d, \psi) \frac{(m+1)cos^m(\phi)}{2\pi} exp(-c(\lambda)L), \tag{1}$$

where $\eta_t$ and $\eta_r$ are the LED efficiency of the transmitter and the conversion efficiency of receiver detector, respectively, $A_{eff}(L,\psi) = \frac{\pi D_r^2 cos(\psi)/4}{\pi(Ltan(\phi_{1/2})+D_t/2)^2}$ represents the equivalent receiving area of the detector, $D_t$ represents the diameter of the collimating lens of the transmitter, $D_r$ represents the diameter of the receiver lens, $m$ is the Lambertian radiation order, $m = \frac{-ln(2)}{ln(cos(\phi_{1/2}))}$, $\phi_{1/2}$ is the half-power emission angle of the LED, $\phi$ is the LED emission angle, $\psi$ is the incidence angle of the detector, and $L$ is the distance of the system.

The channel matrix $\mathbf{H}$ of underwater optical MIMO can be obtained from the calculated channel DC gain, where $\mathbf{H} = \begin{bmatrix} h_{11} & \cdots & h_{1N_t} \\ \vdots & \ddots & \vdots \\ a_{N_r1} & \cdots & a_{N_rN_t} \end{bmatrix}$.

The gain matrix of the underwater optical channel can be obtained through the DC gain coefficient of the above underwater optical channel, and the signal vector at the receiver can be expressed as:

$$\mathbf{y} = \mathbf{Hs} + \mathbf{n}, \tag{2}$$

where $\mathbf{s}$ is the transmitter signal vector, and $\mathbf{n}$ is Gaussian white noise with a mean of 0 and variance of $\sigma_n^2$.

*2.3. Underwater Turbulence and Link Misalignment Channel Model*

When the beam propagates in an underwater environment, the underwater turbulence will cause random fluctuation in the amplitude of the illuminated beam during the propagation process. The random fluctuation of the beam can be approximately equivalent to the multiplicative interference to the signal. The variation coefficient of the illumination amplitude under the effect of turbulence can be simulated by the lognormal distribution probability density function (PDF) [29]:

$$f(\alpha) = \frac{1}{2\alpha\sqrt{2\pi\sigma_\rho^2}} exp(-\frac{(\ln(\alpha) - 2\mu_\rho)^2}{8\sigma_\rho^2}), \tag{3}$$

where $\alpha$ represents the fading coefficient in turbulent environment, which follows an exponential normal distribution, expressed as $\ln(\alpha) \sim N(\mu_\rho, \sigma_\rho^2)$, $\mu_\rho$ and $\sigma_\rho^2$ denote the mean and variance of the normal-distributed. Usually, the scintillation index $\sigma_I^2$ is used to quantify the turbulence strength, which is defined as:

$$\sigma_I^2 = \frac{E[I^2] - E^2[I]}{E^2[I]} = \frac{E[\alpha^2] - E^2[\alpha]}{E^2[\alpha]}, \tag{4}$$

In addition to the influence of turbulence, the underwater optical massive MIMO system will also be affected by the misalignment. The link misalignment error $\triangle x$ can be simulated by the Rayleigh distribution probability density function (PDF) [30]:

$$f(\triangle d) = \frac{\triangle d}{\sigma^2} \exp^{\frac{\triangle d^2}{2\sigma^2}}, \tag{5}$$

where $\triangle d$ is link misalignment error, and $\sigma^2$ is the variance of link misalignment error.

Figure 3 shows the image spot distribution diagram of the transceiver's receiver under the condition of alignment and misalignment. The horizontal offset can be decomposed into two components of parallel $x$ axis and behavior $y$ axis by geometric decomposition method. As shown in Figure 3b, link misalignment will cause the receiver detector to receive multiple light spots simultaneously, leading to enhanced interference between the sub-channels of the system.


**Figure 3.** Image spot distribution diagram at the receiver. (**a**) Transceiver alignment. (**b**) The transceiver link misalignment.

The imaging spot diameter is $2r$, which is exactly equal to the detector side length. The light intensity inside the imaging spot is uniformly distributed. The gap between the different detectors is small enough.

If the above conditions are satisfied, the area covered by the $i$-th imaging spot offset caused by link misalignment in adjacent detectors can be expressed by the following formula:

$$S_i(\triangle x) = r^2 arccos(\frac{r-\triangle x}{r}) - (r-\triangle x)\sqrt{2r(\triangle x) - \triangle x^2}, \quad (6)$$

where $r$ is the radius of imaging spot, $\triangle x = \triangle d/M$, $\triangle x$ is the distance of imaging spot offset, and its value obeys Rayleigh distribution, and $\triangle d$ and $M$ are, respectively, the relative offset distance of the transceiver and the magnification of the imaging lens of the receiver.

Then the interference coefficient value is shown as follows:

$$\hat{h}_i(\triangle x) = h_i \frac{S_i(\triangle x)}{\pi r^2}. \quad (7)$$

By tracing each light path emitted by the LED light source using ZEMAX software, the distribution of light spots imaged by the receiver can be obtained. The simulated system is a 16 × 16 MIMO system compared with the traditional MIMO system, the interference between imaging spots is larger, and the correlation between channels is higher. This paper uses the aspherical imaging lens group as the receiver imaging lens [31]. The aspherical lens can effectively reduce the influence of imaging lens spherical aberration, and using multiple lenses can effectively separate the interference between the image spots of different LEDs. Optical path simulation parameters are shown in Table 1.

**Table 1.** ZEMAX optical path simulation parameters.

| Parameters | Value |
|---|---|
| LED wavelength | 520 nm |
| Number of LEDs | 16 |
| Number of detectors | 16 |
| LED spacing between groups | 300 cm |
| LED spacing within the group | 8 mm |
| LED half-power angle | 17° |
| Communication distance | 4 m |
| Number of trace rays | $10^6$ |
| Detector side length | 3 mm |

The data transmitted by the four LEDs in each group of light sources is encoded using STBC technology, and the four groups transmit four different signals, respectively. To enable the imaging lens properly, it is preferential to separate the light beams between other light source groups; the space between the four groups should be much larger than the LED space inside each group of light sources. The receiver detector can divide the received optical signal into four large light spots through the imaging lens, and each large light spot covers multiple detector arrays.

Figure 4 shows the distribution of imaging light spots at the receiver. The spacing between each spot is about 3.2 mm, and the imaging lens groups can effectively separate the beam between different LEDs. Figure 5 shows the channel matrix of the underwater optical massive MIMO system obtained by ZEMAX. Since the underwater optical MIMO system uses an imaging lens at the receiver, the light spots formed by different LEDs at the receiver are separated by the imaging lens for the underwater optical MIMO system. The diagonal elements of the channel matrix are much larger than the off-diagonal elements.

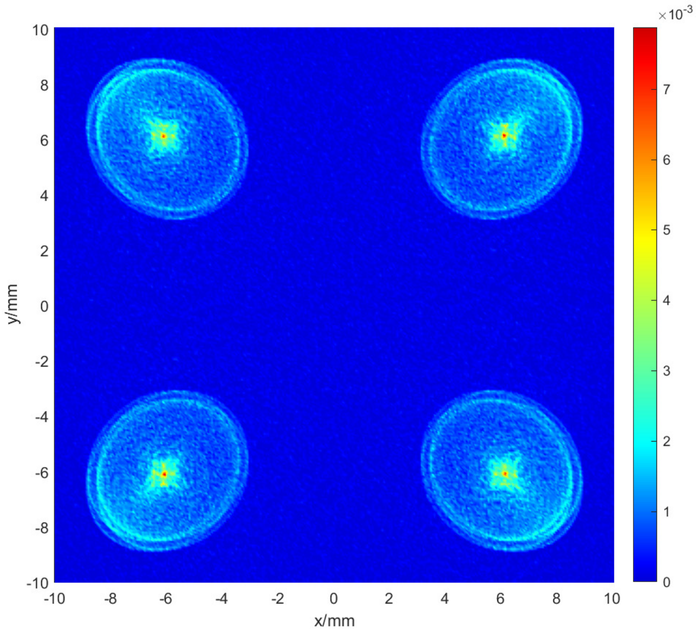


**Figure 4.** Image spot pattern at the receiver.

$$
\mathbf{H}=\left[\begin{array}{cccc|cccc|cccc|cccc}
80.88959 & 16.42643 & 51.7462 & 437.5291 & 3.922084 & 2.53172 & 7.676951 & 9.082085 & 8.758051 & 4.441867 & 4.965786 & 7.740248 & 3.941051 & 2.44609 & 4.397589 & 5.060084 \\
74.93837 & 24.95793 & 77.0644 & 382.4088 & 4.177742 & 3.197408 & 7.923791 & 8.175575 & 9.613385 & 5.099326 & 4.396594 & 9.019573 & 2.731964 & 2.267827 & 2.913971 & 6.137096 \\
56.92243 & 17.14421 & 79.91177 & 443.3921 & 3.847394 & 3.538015 & 7.154806 & 8.324098 & 7.817404 & 4.978755 & 3.577599 & 8.949272 & 3.669157 & 2.212865 & 3.914991 & 6.316138 \\
39.71893 & 15.3035 & 54.71811 & 422.6583 & 3.719739 & 2.569376 & 7.754294 & 6.836185 & 7.100477 & 5.097915 & 4.769988 & 8.316189 & 3.080785 & 2.787921 & 2.870246 & 6.53007 \\
\hline
7.90186 & 8.253459 & 3.452044 & 3.546528 & 498.0096 & 59.65314 & 20.19507 & 50.30214 & 5.551396 & 4.134619 & 2.397137 & 2.923429 & 7.963414 & 4.720248 & 3.545298 & 7.829042 \\
8.179833 & 7.065001 & 4.351382 & 3.027446 & 390.8742 & 80.66792 & 19.54562 & 42.53321 & 6.254451 & 3.00171 & 2.233808 & 3.183376 & 11.07257 & 4.12204 & 5.085036 & 8.843719 \\
8.219028 & 7.315205 & 3.897756 & 3.301201 & 434.3137 & 59.40322 & 29.48649 & 63.63582 & 4.958228 & 3.883233 & 2.658336 & 3.477513 & 10.32694 & 4.874725 & 5.052451 & 6.945624 \\
9.249723 & 7.133009 & 3.711025 & 3.683679 & 358.892 & 44.36158 & 20.156 & 69.28534 & 5.044864 & 3.961726 & 2.836006 & 3.597471 & 8.164327 & 4.122354 & 4.909153 & 6.964272 \\
\hline
4.924486 & 6.98711 & 10.4862 & 4.471014 & 2.305747 & 3.921721 & 6.254973 & 3.320142 & 25.91576 & 66.55678 & 327.1984 & 71.09661 & 3.696021 & 3.870271 & 6.868137 & 7.262227 \\
4.447544 & 6.331851 & 9.106271 & 4.617022 & 2.081271 & 3.491862 & 5.29969 & 3.594907 & 24.09026 & 76.2922 & 416.5778 & 59.64781 & 4.151676 & 3.82365 & 6.621294 & 8.467433 \\
4.353118 & 8.924682 & 8.747252 & 4.944418 & 2.634092 & 2.383247 & 4.156733 & 4.275208 & 17.24545 & 58.92139 & 481.3178 & 65.70325 & 3.430088 & 3.160065 & 8.016751 & 6.28024 \\
4.747865 & 7.450951 & 8.894625 & 3.739594 & 2.469012 & 3.180537 & 4.581116 & 3.995945 & 19.69647 & 40.51259 & 385.7889 & 75.58883 & 4.128231 & 3.642276 & 8.202833 & 7.1511 \\
\hline
4.416821 & 4.236818 & 2.645684 & 2.715538 & 4.406803 & 6.847417 & 5.547001 & 4.587582 & 7.165933 & 6.326391 & 2.979703 & 3.791993 & 84.57091 & 443.2647 & 54.72195 & 19.89784 \\
3.046682 & 6.262106 & 2.844654 & 2.614769 & 4.274322 & 9.563758 & 8.761328 & 4.817489 & 5.765724 & 6.38221 & 4.20113 & 3.593593 & 67.25554 & 512.4201 & 60.53263 & 20.80128 \\
3.694526 & 5.100497 & 3.565642 & 2.935921 & 4.56244 & 9.302183 & 9.682791 & 4.638508 & 6.927579 & 9.562167 & 3.044972 & 3.958494 & 59.101 & 416.6573 & 85.12787 & 19.97941 \\
3.210235 & 5.686287 & 2.55666 & 2.162918 & 3.150722 & 8.204825 & 10.71954 & 5.511966 & 8.433511 & 7.493169 & 4.19623 & 4.217274 & 60.85465 & 397.3787 & 78.52175 & 31.04434
\end{array}\right]\times 10^{8}
$$

**Figure 5.** Channel gain matrix with transmitter and receiver aligned.

Through the imaging lens at the receiver and the EGC combining technology, the system can be equivalent to a 4 × 4 MIMO multiplexing system. The imaging lens and the EGC technology can reduce the dimension of the underwater optical massive MIMO system. It can be observed from the channel matrix shown in Figure 5 that the 16 × 16 matrix is divided into 16 channel matrices. The imaging lens makes the correlation between each channel matrix low, which can be equivalently expressed as follows:

$$\mathbf{H}=\mathbf{H}_1 \bigotimes \mathbf{H}_2, \tag{8}$$

where $\mathbf{H}_1$ is the channel matrix of the group using STBC coding, and $\mathbf{H}_2$ is the channel matrix between different groups. Due to the short distance between the LEDs in the light source group using STBC coding, the imaging lens cannot separate the beams of other LEDs, so $\mathbf{H}_1$ can be regarded as a matrix with a high correlation of spot aliasing, and $\mathbf{H}_2$ is the channel matrix between different groups. The imaging lens has a better beam-separation effect between other light source groups, so the correlation of matrix $\mathbf{H}_2$ is low. Its diagonal elements are much larger than off-diagonal elements. The channel matrix $\mathbf{H}$ with low correlation between the matrix blocks on the diagonal and the matrix blocks on the off-diagonal is obtained by calculating the Kronecker product of $\mathbf{H}_1$, $\mathbf{H}_2$. The dimensionality reduction processing of the system by the block can effectively reduce the channel correlation.

The correlation of the channel gain matrix $\mathbf{H}$ can be represented by the channel condition number $k = ||\mathbf{H}||||\mathbf{H}^{-1}||$ [20]. Figure 6 shows the relationship between the number of channel gain matrix conditions and the offset generated by the horizontal offset of the receiver and transmitter. The condition number of $\mathbf{H}$ increases with the relative offset of link misalignment error. When the number of channel conditions is small, the interference between the signals at the receiver is small and can be obtained by direct demodulation. With the increase of the degree of link misalignment, the number of channel gain matrix conditions also increases. When the number of channel conditions is large, the interference between signals is high, and the system cannot directly demodulate signals.

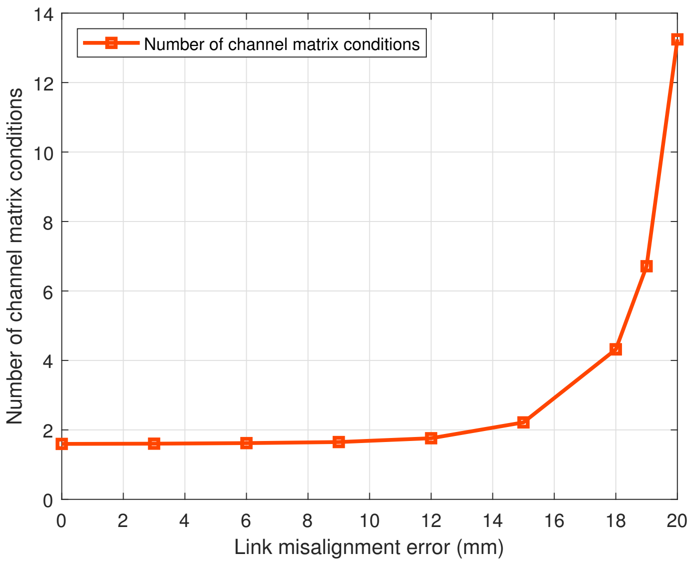


**Figure 6.** The conditions number of $\mathbf{H}$ versus the link misalignment error $\triangle x$.

Through the imaging lens at the receiving end, the light beams from different LEDs are separated, and the elements on the diagonal of the channel matrix are much larger than those on the non-diagonal. At this time, the interference between different LED beams is mainly caused by spot mobility caused by link misalignment. Different directions of spot mobility will cause the detector to be interfered with by other spots. Taking Figure 3b as an example, the channel matrix can be represented as follows:

$$\mathbf{H}(\triangle x) = \begin{bmatrix} h_{11} & & & & \\ h_{11}\frac{S_1(\triangle x)}{\pi r^2} & h_{22} & & & \\ & & \ddots & & \\ & & h_{(N_t-2)(N_r-2)}\frac{S_{N_t-2}(\triangle x)}{\pi r^2} & h_{(N_t-1)(N_r-1)} & \\ & & & h_{(N_t-1)(N_r-1)}\frac{S_{N_t-1}(\triangle x)}{\pi r^2} & h_{N_tN_r} \end{bmatrix}, \tag{9}$$

where the value of the ignored element in the channel matrix **H** after the beam is separated by the imaging lens is much smaller than the value that is not ignored. $S_i$ represents the size of the image spot area of the $i$ LED on the detector at the receiver. $N_t$ and $N_r$ represent the number of LEDs at the transmitter and the number of the detector at the receiver.

Considering the joint effect of turbulence and link misalignment, the turbulence random attenuation coefficient $\alpha$ is substituted into Equation (9), and the channel matrix can be expressed as follows:

$$\hat{\mathbf{H}}(\triangle x) = \alpha \mathbf{H}(\triangle x). \tag{10}$$

## 3. Improve Order Successive Interference Cancellation Algorithm Based on Partition STBC

In this paper, the Alamouti STBC algorithm is used to substantially reduce the impact of turbulence on system reliability. EGC technology can be adopted for signal combining processing at the receiver [27] to further reduce the complexity of the receiver component of the system.

STBC-EGC technology can effectively reduce the complexity of adopting the STBC coding system. This paper applies STBC-EGC technology to the underwater optical massive MIMO system, improving system reliability and communication capacity through block processing.

In the actual underwater environment, the underwater optical massive MIMO system is not only affected by the random attenuation of the optical signal caused by turbulence but also affected by the imaging spot deviation of the receiving end, caused by the misalignment of the receiving end. The correlation between system sub-channels increases with the increase of link misalignment errors. In case of high correlation of sub-channels, the system cannot demodulate the signal directly, so the MIMO detection algorithm is needed for signal detection.

To eliminate interference between array signals, the order successive interference cancellation (OSIC) algorithm is suitable for canceling interference between signals successively. The channel demodulation sequence of the traditional OSIC algorithm is mainly sorted according to receiver signal power.

Under the combined effect of underwater turbulence and link misalignment, receiver signals are arranged in power levels. The channel matrix of Equation (10) is used to sum the elements in each row of the matrix and sort them. The following formula can express the sorting index of the OSIC algorithm:

$$\mathbf{I}_{index} = argmax \begin{bmatrix} h_{11} + h_{12} \cdots + h_{1N_r} \\ \vdots \\ h_{N_tN_r} + h_{N_t1} \cdots + h_{N_tN_r-1} \end{bmatrix} = argmax \begin{bmatrix} h_{11} \\ h_{11}\frac{S_1}{\pi r^2} + h_{22} \\ \vdots \\ h_{(N_t-2)(N_r-2)}\frac{S_{N_t-2}}{\pi r^2} + h_{(N_t-1)(N_r-1)} \\ h_{(N_t-1)(N_r-1)}\frac{S_{N_t-1}}{\pi r^2} + h_{N_tN_r} \end{bmatrix}. \tag{11}$$

As shown in Equation (11), the sorting index of OSIC will preferably demodulate signals with higher receiver signal power. For the underwater optical massive MIMO system under the combined effect of underwater turbulence and link misalignment, OSIC demodulation priority is given to the signals with the most interference from adjacent beams. Therefore, based on the traditional OSIC algorithm, we propose an I-OSIC algorithm based on minimum permutation of interference. Channel matrix **H** is obtained through the channel estimation algorithm. The difference processing of diagonal elements in each row of elements in channel matrix **H** and other elements is performed to obtain $\triangle\mathbf{H}$. $\triangle\mathbf{H}$ is expressed as follows:

$$\triangle\mathbf{H} = argmax\begin{bmatrix} h_{11} - h_{12}\cdots - h_{1N_r} \\ \vdots \\ h_{N_tN_r} - h_{N_t1}\cdots - h_{N_tN_r-1} \end{bmatrix} = argmax\begin{bmatrix} h_{11} \\ h_{22} - h_{11}\frac{S_1}{\pi r^2} \\ \vdots \\ h_{(N_t-1)(N_r-1)} - h_{(N_t-2)(N_r-2)}\frac{S_{N_t-2}}{\pi r^2} \\ h_{N_tN_r} - h_{(N_t-1)(N_r-1)}\frac{S_{N_t-1}}{\pi r^2} \end{bmatrix}. \quad (12)$$

Formula (12) is used as the signal demodulation sequence index, and the signal with the least interference can be preferably selected for demodulation.

## 4. Simulation Result Analysis

Figure 7 shows the relationship curve between the condition number of the channel matrix and the degree of link misalignment under the combined effect of weak underwater turbulence and link misalignment. With the increase of the relative offset of the transmitter and receiver, the condition number of the channel matrix also increases. By dividing the underwater optical massive MIMO system into blocks and using the diversity technique, the correlation of the channel matrix can be effectively reduced. In contrast, the dimension of the channel matrix is reduced.

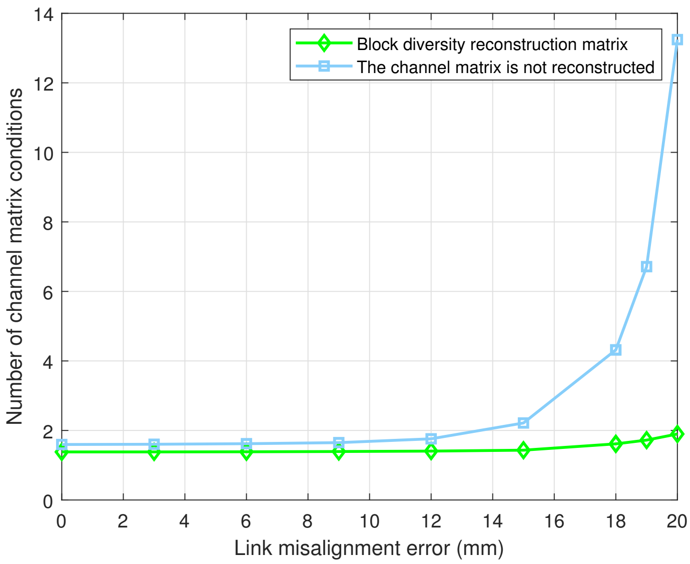


**Figure 7.** The conditions number of $\mathbf{H}$ versus the link misalignment error $\triangle x$ in turbulent environment.

After using the block diversity technique, the condition number of the channel matrix is reduced, but the channel correlation is still increasing with the increase of the link misalignment error. In addition, in the case of large link misalignment, part of the received optical signal will be lost. Figure 8 shows the distribution of imaging spots under different link misalignment degrees. By applying diversity techniques to the underwater optical massive MIMO system blocks, the imaging within the same diversity combination can be combined into a large spot. Figure 8a shows the spot distribution when the link misalignment degree is small. Due to the adopted block diversity technology, the correlation between sub-channels in the same diversity combination does not need to be considered. Only the correlation between different diversity blocks needs to be considered, so the dimension of the channel matrix of the underwater optical massive MIMO system can be reduced, and the correlation between sub-channels is further reduced.


**Figure 8.** Schematic diagram of imaging spot distribution under different link misalignments. (**a**) The degree of link misalignment is small. (**b**) The degree of link misalignment is large.

Figure 9 shows the BER curves of systems with different diversity orders in a weak turbulent environment. As shown in Figure 9, when the BER of 4 × 4 STBC encoding STBC is 2 × 2,the SNR of the 4 × 4 STBC encoding system is improved by about 5 dB compared with the 2 × 2 STBC encoding system. The higher the diversity order, the higher the system's resistance to fading caused by turbulence.

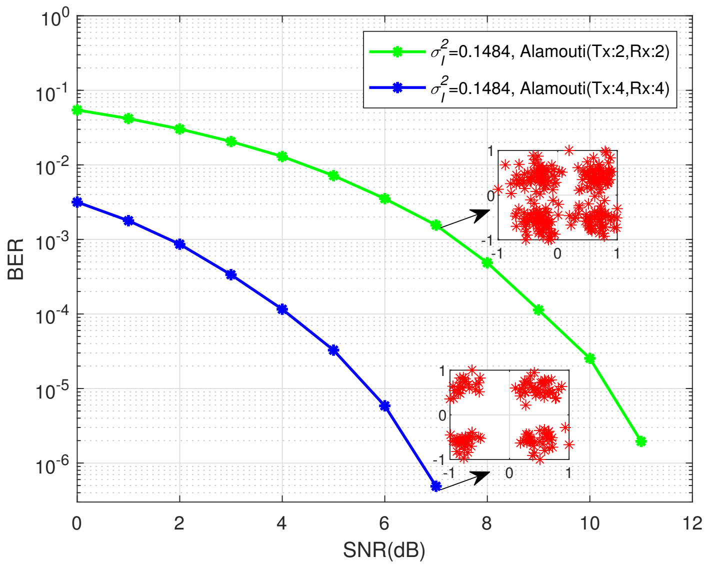


**Figure 9.** BER curves of systems with different diversity orders under weak turbulence conditions.

Figure 10 shows the BER curves of the 4 × 4 STBC coding system under different turbulent current environments. The multiplexing system using part of the 4 × 4 STBC coding has an SNR of about 10 dB in a strong turbulent environment. This system is based on an underwater optical massive MIMO system, and some communication links adopt diversity technology, further improving the system's effectiveness by ensuring the system's reliability.

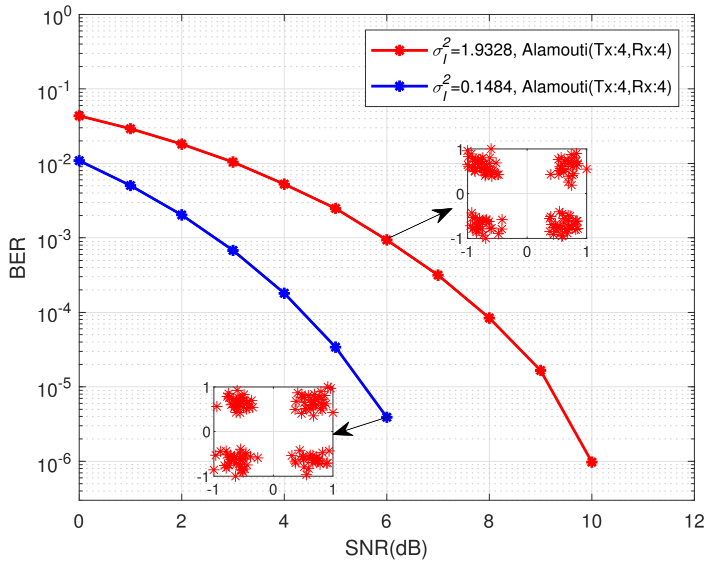


**Figure 10.** BER curves of 4 × 4 STBC coding system under different turbulent environments.

This paper uses 4 QAM ACO-OFDM modulation to simulate the underwater optical massive MIMO system. The main simulation parameters are shown in Table 2. The simulation environment is a coastal seawater environment, and its underwater visible light attenuation coefficient is about 0.15.

**Table 2.** Simulation parameters of underwater optical massive MIMO system.

| Parameters | Value |
|---|---|
| Subcarrier number | 128 |
| Number of OFDM symbols | 1000 |
| Diameter of the receiving lens | 30 mm |
| LED spacing within the group | 8 mm |
| Attenuation coefficient of underwater visible light | 0.15 |
| Communication distance | 4 m |
| Receiver detector conversion efficiency | 0.95 |
| Transmitter LED conversion efficiency | 0.1289 |

Figure 11 shows the simulation diagram of the BER of the system when the link misalignment error is small. Figure 12 shows the simulation diagram of the BER of the system when the link misalignment error is large. As the horizontal deviation error caused by the misalignment of the receiver and transmitter increases, the interference between the two adjacent columns of light spots also increases. As the OSIC algorithm based on minimum interference sorting is used to detect and sort based on the minimum link misalignment interference criterion, when the link misalignment error is small, the diagonal element of channel matrix H is much larger than the non-diagonal element. At this time, Equation (12) is simplified to sort and detect according to the size of the diagonal element. Therefore, when the horizontal migration error is small, the OSIC algorithm based on minimum disturbance sorting and the I-OSIC algorithm have similar BER performance.

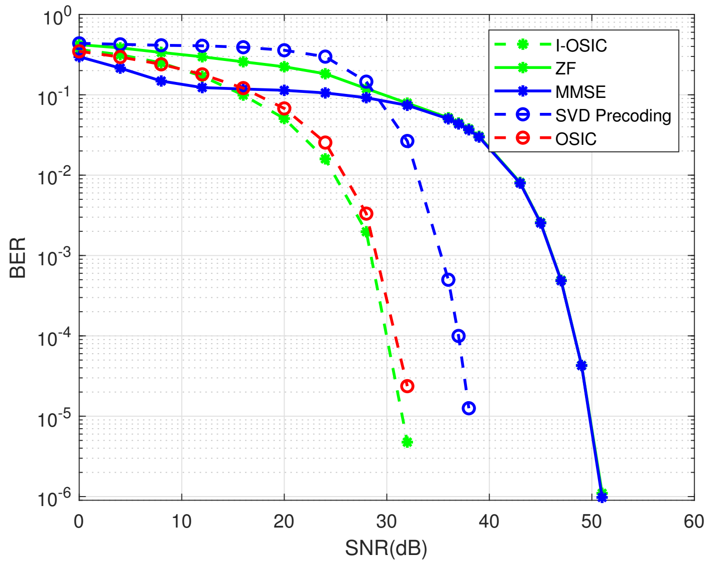


**Figure 11.** Receiver and transmitter aligned system BER performance.

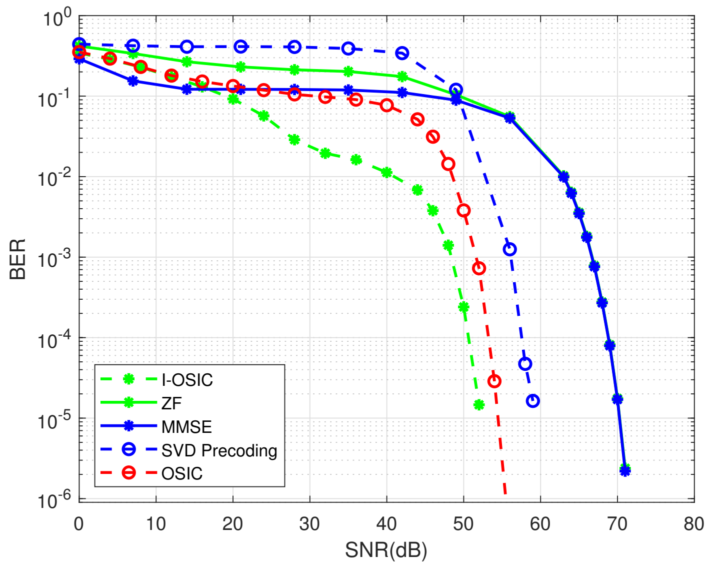


**Figure 12.** System BER performance when the link misalignment error is 18 mm.

The channel correlation also increases with the relative offset error of the receiver and transmitter. At this time, SVD precoding has limited improvement on the system error performance in the poor channel environment. Aiming at the problem of misalignment of the receiver and transmitter, the I-OSIC algorithm is proposed in this paper. Compared with the traditional OSIC algorithm based on receiver power sorting, the BER performance of the system is improved to a certain extent.

As shown in Figure 13, the system BER varies with the link misalignment error. When SNR is 13 dB, the I-OSIC algorithm has the best BER performance under the same link misalignment error. Compared with the traditional MIMO detection algorithm, the I-OSIC algorithm has better detection performance under the condition of link misalignment.

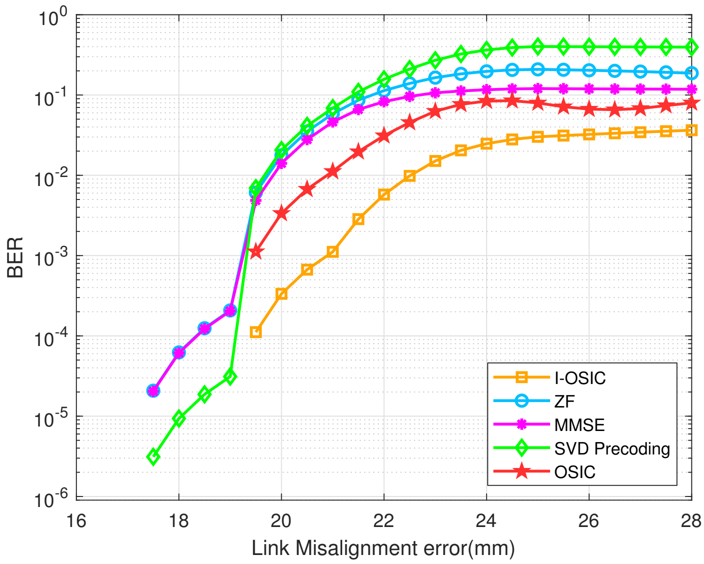


**Figure 13.** The system BER versus the link misalignment error when SNR is 30 dB.

## 5. Conclusions

This paper studies the enhancement of sub-channel correlation caused by the combined effect of underwater turbulence and link misalignment for the transmission of optical signals in the underwater optical massive MIMO systems. Considering the combined effects of turbulence and link misalignment separately, the I-OSIC algorithm based on block STBC interference minimum ordering is proposed. The STBC technology can effectively resist the random fading of optical signals in turbulent environments. However, to reduce the channel correlation under link misalignment, all antennas in the system need diversity techniques, consequently leading toward the waste of communication resources. The I-OSIC algorithm based on block STBC is proposed in this paper, which divides massive MIMO systems into different groups and uses diversity technologies, respectively. The I-OSIC algorithm can adopt other receiver signal-sequencing detection schemes according to the different degrees of link misalignment. Even when the degree of link misalignment is large, I-OSIC can adopt the receiver signal-sequencing detection scheme with minimum interference, according to the degree of link misalignment, to reduce the correlation of the channel matrix and improve the BER performance of the system.

The I-OSIC algorithm proposed in this paper mainly aims at the light spot migration caused by link misalignment, so that the same detector will receive light signals from multiple light spots. However, when the link misalignment is large enough, the light spot will deviate from the receiving limit range of the detector. At this time, the detection algorithm can no longer solve this problem, so it is necessary to solve this problem by other means, such as increasing the receiver field angle, increasing the detector array, etc.

**Author Contributions:** Conceptualization and channel modeling under the combined effects of underwater turbulence and link misalignment, J.F. and K.Z.; methodology for resist random fading of turbulence in underwater optical communication K.Z., Y.L. and J.F.; formal analysis, K.Z. and S.A.H.M.; investigation, K.Z. and J.F.; resources, K.Z., Y.L., S.A.H.M. and J.F.; data curation, K.Z. and J.F.; writing—original draft preparation, K.Z. and J.F.; writing—review and editing, K.Z., J.F. and S.A.H.M.; visualization, K.Z.; supervision, K.Z. and J.F.; project administration, K.Z., Y.L. and J.F.; funding acquisition, Y.L. and J.F. All authors have read and agreed to the published version of the manuscript.

**Funding:** This research was funded by the National Natural Science Foundation of China under grant (62261009), the Guangxi Natural Science Foundation, China (2022GXNSFDA035070), Ministry of Education Key Laboratory of Cognitive Radio and Information Processing (CRKL200106) and Innovation Project of Guangxi Graduate Education (YCSW2022288).

**Institutional Review Board Statement:** Not applicable.

**Informed Consent Statement:** Not applicable.

**Data Availability Statement:** The data presented in this study are available on request from the corresponding author. The data are not publicly available due to requirements of internal authorization with the experiment team.

**Conflicts of Interest:** The authors declare no conflict of interest.

## References


1. Nie, J.; Tian, L.; Wang, H.; Chen, L.; Li, Z.; Yue, S.; Zhang, Z.; Yang, H. Adaptive beam shaping for enhanced underwater wireless optical communication. *Opt. Express* **2021**, *29*, 26404–26417. [CrossRef]
2. Shi, C.; Dubois, M.; Wang, Y.; Zhang, X. High-speed acoustic communication by multiplexing orbital angular momentum. *Proc. Natl. Acad. Sci. USA* **2017**, *114*, 7250–7253. [CrossRef] [PubMed]
3. Ali, M.F.; Jayakody, D.N.K.; Chursin, Y.A.; Affes, S.; Dmitry, S. Recent Advances and Future Directions on Underwater Wireless Communications. *Arch. Comput. Methods Eng.* **2020**, *27*, 1379–1412. [CrossRef]
4. Ryecroft, S.; Shaw, A.; Fergus, P.; Kot, P.; Hashim, K.; Moody, A.; Conway, L. A First Implementation of Underwater Communications in Raw Water Using the 433 MHz Frequency Combined with a Bowtie Antenna. *Sensors* **2019**, *19*, 1813. [CrossRef]
5. Esmaeili, H.; Hakami, V.; Minaei Bidgoli, B.; Shokouhifar, M. Application-specific clustering in wireless sensor networks using combined fuzzy firefly algorithm and random forest. *Expert Syst. Appl.* **2022**, *210*, 118365. [CrossRef]
6. Shokouhifar, M. Swarm intelligence RFID network planning using multi-antenna readers for asset tracking in hospital environments. *Comput. Netw.* **2021**, *198*, 108427. [CrossRef]
7. Aboelala, O.; Lee, I.E.; Chung, G.C. A Survey of Hybrid Free Space Optics (FSO) Communication Networks to Achieve 5G Connectivity for Backhauling. *Entropy* **2022**, *24*, 1573. [CrossRef] [PubMed]
8. Pompili, D.; Akyildiz, I.F. Overview of networking protocols for underwater wireless communications. *IEEE Commun. Mag.* **2009**, *47*, 97–102. [CrossRef]
9. Hanson, F.; Radic, S. High bandwidth underwater optical communication. *Appl. Opt.* **2008**, *47*, 277–283. [CrossRef]
10. Huang, J.; Li, C.; Lei, Y.; Yang, L.; Xiang, Y.; Curto, A.G.; Li, Z.; Guo, L.; Cao, Z.; Hao, Y.; et al. A 20-Gbps Beam-Steered Infrared Wireless Link Enabled by a Passively Field-Programmable Metasurface. *Laser Photonics Rev.* **2020**, *15*, 2000266. [CrossRef]
11. Schirripa Spagnolo, G.; Cozzella, L.; Leccese, F. Underwater Optical Wireless Communications: Overview. *Sensors* **2020**, *20*, 2261. [CrossRef] [PubMed]
12. Oubei, H.M.; Duran, J.R.; Janjua, B.; Wang, H.-Y.; Tsai, C.-T.; Chi, Y.-C.; Ng, T.K.; Kuo, H.-C.; He, J.-H.; Alouini, M.-S.; et al. 4.8 Gbit/s 16-QAM-OFDM transmission based on compact 450-nm laser for underwater wireless optical communication. *Opt. Express* **2015**, *23*, 23302–23309. [CrossRef] [PubMed]
13. Wu, T.-C.; Chi, Y.-C.; Wang, H.-Y.; Tsai, C.-T.; Lin, G.-R. Blue Laser Diode Enables Underwater Communication at 12.4 Gbps. *Sci. Rep.* **2017**, *7*, 40480. [CrossRef] [PubMed]
14. Xu, J.; Song, Y.; Yu, X.; Lin, A.; Kong, M.; Han, J.; Deng, N. Underwater wireless transmission of high-speed QAM-OFDM signals using a compact red-light laser. *Opt. Express* **2016**, *24*, 8097–8109. [CrossRef] [PubMed]
15. Tian, P.; Liu, X.; Yi, S.; Huang, Y.; Zhang, S.; Zhou, X.; Hu, L.; Zheng, L.; Liu, R. High-speed underwater optical wireless communication using a blue GaN-based micro-LED. *Opt. Express* **2017**, *25*, 1193–1201. [CrossRef]
16. Han, B.; Zhao, W.; Zheng, Y.; Meng, J.; Wang, T.; Han, Y.; Wang, W.; Su, Y.; Duan, T.; Xie, X. Experimental demonstration of quasi-omni-directional transmitter for underwater wireless optical communication based on blue LED array and freeform lens. *Opt. Commun.* **2019**, *434*, 184–190. [CrossRef]
17. Xu, K.; Yu, H.; Zhu, Y.-J. Channel-Adapted Spatial Modulation for Massive MIMO Visible Light Communications. *IEEE Photonics Technol. Lett.* **2016**, *28*, 2693–2696. [CrossRef]
18. Biswas, S.; Masouros, C.; Ratnarajah, T. Performance Analysis of Large Multiuser MIMO Systems With Space-Constrained 2-D Antenna Arrays. *IEEE Trans. Wirel. Commun.* **2016**, *15*, 3492–3505. [CrossRef]
19. Joung, J.; Kurniawan, E.; Sun, S. Channel Correlation Modeling and its Application to Massive MIMO Channel Feedback Reduction. *IEEE Trans. Veh. Technol.* **2017**, *66*, 3787–3797. [CrossRef]
20. Karunatilaka, D.; Zafar, F.; Kalavally, V.; Parthiban, R. LED Based Indoor Visible Light Communications: State of the Art. *IEEE Commun. Surv. Tutor.* **2015**, *17*, 1649–1678. [CrossRef]
21. Wang, T.Q.; Sekercioglu, Y.A.; Armstrong, J. Analysis of an Optical Wireless Receiver Using a Hemispherical Lens with Application in MIMO Visible Light Communications. *J. Light. Technol.* **2013**, *31*, 1744–1754. [CrossRef]
22. Chen, T.; Liu, L.; Tu, B.; Zheng, Z.; Hu, W. High-Spatial-Diversity Imaging Receiver Using Fisheye Lens for Indoor MIMO VLCs. *IEEE Photonics Technol. Lett.* **2014**, *26*, 2260–2263. [CrossRef]
23. Wei, J.; Gong, C.; Huang, N.; Xu, Z. Channel Modeling and Signal Processing for Array-Based Visible Light Communication System Under Link Misalignment. *IEEE Photonics J.* **2022**, *14*, 1–10. [CrossRef]
24. Jamali, M.V.; Salehi, J.A.; Akhoundi, F. Performance Studies of Underwater Wireless Optical Communication Systems with Spatial Diversity: MIMO Scheme. *IEEE Trans. Commun.* **2017**, *65*, 1176–1192. [CrossRef]

25. Sharifzadeh, M.; Ahmadirad, M. Performance analysis of underwater wireless optical communication systems over a wide range of optical turbulence. *Opt. Commun.* **2018**, *427*, 609–616. [CrossRef]
26. Bhatnagar, M.R.; Anees, S. On the Performance of Alamouti Scheme in Gamma-Gamma Fading FSO Links with Pointing Errors. *IEEE Wirel. Commun. Lett.* **2015**, *4*, 94–97. [CrossRef]
27. Shi, J.; Huang, X.; Wang, Y.; Tao, L.; Chi, N. Improved performance of a high speed 2 × 2 MIMO VLC network based on EGC-STBC. In Proceedings of the 2015 European Conference on Optical Communication (ECOC), Valencia, Spain, 27 September–1 October 2015; pp. 1–3.
28. Wang, P.; Li, C.; Xu, Z. A Cost-Efficient Real-Time 25 Mb/s System for LED-UOWC: Design, Channel Coding, FPGA Implementation, and Characterization. *J. Light. Technol.* **2018**, *36*, 2627–2637. [CrossRef]
29. Ijeh, I.C.; Khalighi, M.A.; Elamassie, M.; Hranilovic, S.; Uysal, M. Outage probability analysis of a vertical underwater wireless optical link subject to oceanic turbulence and pointing errors. *J. Opt. Commun. Netw.* **2022**, *14*, 439–453. [CrossRef]
30. Sandalidis, H.G.; Tsiftsis, T.A.; Karagiannidis, G.K. Optical Wireless Communications with Heterodyne Detection Over Turbulence Channels with Pointing Errors. *J. Light. Technol.* **2009**, *27*, 4440–4445. [CrossRef]
31. Li, S.-B.; Gong, C.; Wang, P.; Xu, Z. Lens design for indoor MIMO visible light communications. *Opt. Commun.* **2017**, *389*, 224–229. [CrossRef]